tunneling current caused instability of the tip as evidenced by the appearance of a high-frequency noise in the scan signal.

Our X-ray diffraction results indicate that the orientation of the annealed Pt film is predominantly ⟨111⟩. This is consistent with the fact that the f.c.c. Pt {111} plane has the same symmetry as the underlying graphite (0001) basal plane, therefore appearing to be the favourite plane for epitaxic growth. This result is in disagreement with some of the previous studies of carbon on a Pt surface (Mundschau & Vanselow, 1985; Vanselow & Mundschau, 1986) and Pt on a graphite surface (Santiesteban *et al.*, 1983). In field emission microscopy (FEM) studies, Mundschau & Vanselow (1985; Vanselow & Mundschau, 1986) found that carbon islands preferentially form on the {110} area of Pt. Santiesteban *et al.* deposited Pt particles on a graphite surface and found that about 60% of the Pt particles have (110) faces in contact with the basal plane of graphite. The different orientation of our Pt film on graphite could be due to the difference in preparation methods. In the present study, the Pt coverage started at 100% while in the other studies the starting coverage was much lower. This difference in Pt coverage could play a major role in determining the orientation of the epitaxic layer (Pashley, 1965). In the present study, the metal films were deposited on newly cleaved graphite in a high vacuum system while in Santiesteban's work, no continuous film was formed on graphite and the metal particles were formed by impregnation of $H_2PtCl_6.6H_2O$ followed by reduction in H_2. Understandably, the cleanness of the metal-graphite interface was very different between our sample and Santiesteban's.

We have noticed that ambient atmosphere could have significant effects on the annealing process. A different atmosphere could result in a different crystallization temperature and even a different orientation of the metal film. Further study will follow to investigate the influence of ambient gas on the annealing process. In addition, the azimuthal relation of the Pt film with the substrate will be revealed in future studies.

The last point that we want to raise is a possible usefulness of the crystallized Pt thin film formed in the present study. On a surface such as that shown in Fig. 4 there are varieties of structural features like terraces, edges and corners *etc.* The presence of these features makes the Pt film a candidate for a model catalyst which has properties between single-crystal catalysts due to its richness in surface features. Yet the thin film is clean and, most importantly, can be characterized by using STM and possibly STS (scanning tunneling spectroscopy) to a near atomic scale. A study of the catalytic properties of the thin film is certainly worthwhile.

We thank Dr K. Chang for carrying out the X-ray diffraction measurement.

References

BINNIG, G., ROHRER, H., GERBER, CH, & WEIBEL, E. (1982*a*). *Appl. Phys. Lett.* **40**, 178-180.
BINNIG, G., ROHRER, H., GERBER, CH. & WEIBEL, E. (1982*b*). *Phys. Rev. Lett.* **49**, 57-61.
CHIDSEY, C. E. D., LOIACONO, D. N., SLEATOR, T. & NAKAHARA, S. (1988). *Surf. Sci.* **200**, 45-66
ELROD, S. A., BRYANT, A., DE LOZANNE, A. L., PARK, S., SMITH, D. & QUATE, C. F. (1986). *J. Res. Dev.* **30**(4), 387-394.
GOETHWL, P. J. & YANG, R. T. (1986). *J. Catal.* **101**, 342-351.
HALLMARK, V. M., CHIANG, S., RAVOLT, J. F., SWALEN, J. D. & WILSON, R. J. (1989). *Phys. Rev. Lett.* **59**(25), 2879-2882.
KOMIYAMA, M., MORITA, S. & MIKOSHIBA, N. (1988). *J. Microsc.* **152**(1), 197-203.
MUNDSCHAU, M. & VANSELOW, R. (1985). *Surf. Sci.* **169**, 23-36.
PASHLEY, D. W. (1965). *Adv. Phys.* **14**, 327-416.
SANTIESTEBAN, J., FUENTES, S. & YACAMAN, M. J. (1983). *J. Mol. Catal.* **20**, 213-231.
SOMORJAI, G. A. (1981). *Chemistry in Two Dimensions: Surfaces.* Ithaca, NY: Cornell Univ. Press.
VANSELOW, R. & MUNDSCHAU, M. (1986). *Surf. Sci.* **176**, 701-708.

Acta Cryst. (1991). A**47**, 21-29

A Model Study of the κ-Refinement Procedure for Fitting Valence Electron Densities

BY A. S. BROWN AND M. A. SPACKMAN

Department of Chemistry, University of New England, Armidale 2351, *New South Wales, Australia*

(*Received* 26 *April* 1990; *accepted* 9 *August* 1990)

Abstract

Monopole electron-density deformations for first- and second-row atoms are obtained using Hirshfeld partitioning of near Hartree-Fock-limit electron densities for 28 diatomics. The κ-refinement model [Coppens, Guru Row, Leung, Stevens, Becker & Yang (1979). *Acta Cryst.* A**35**, 63-72] is applied to these monopole deformations and its success in modelling them is gauged by means of deformation

0108-7673/91/010021-09$03.00

radial distribution plots, $r^2\Delta\rho(r)$, and κ and charge-transfer values. The κ-refinement procedure proves to be remarkably successful in modelling the monopole deformations in this work. This in large part explains the successful application of the κ-refinement model to X-ray diffraction data, where it is capable of yielding an excellent point-charge model of the electrostatic potential in molecules and crystals.

1. Introduction

Multipole refinement of accurate X-ray diffraction data is now a more or less routine procedure for obtaining more quantitative information on electron distributions than can be derived from electron-density maps. It is the method of choice, if not necessity, in virtually all recent electron-density analyses (*e.g.* see Coppens, 1989). There are, however, limitations on the applicability of such an analysis. These include the exceptional demands it places on the X-ray data, and the large number of additional parameters per atom which must be included in the least-squares-refinement procedure. It is therefore not surprising that recent work on the nucleotide 2′-deoxycytidine-5′-monophosphate (Pearlman & Kim, 1985) resorted to a truncated version of this multipole refinement procedure, a monopole model.

Monopole models allow the estimation of atomic net charges, and often, but not always, the resultant expansion or contraction of the valence-electron distribution. Such models are not new, and were in fact used in the first attempts to extract quantitative information on electron distributions from X-ray data. Of the different strategies used, the *L*-shell projection method (Stewart, 1970; Coppens, Pautler & Griffin, 1971) and projection into standard spherical atoms (Yanez, Stewart & Pople, 1978; Yanez & Stewart, 1978) did not explicitly allow for changes in the shape of the valence shell associated with repopulation. The κ-refinement procedure (Coppens, Guru Row, Leung, Stevens, Becker & Yang, 1979), on the other hand, incorporates expansion and contraction of individual atomic valence electron densities, in addition to electron redistribution, and it is this simple model (two parameters per atom) which we analyse in some detail in this work. The κ-refinement model has been frequently used in the past decade for the determination of atomic charges from X-ray diffraction data. Major applications of κ-refinement results have been the determination of molecular multipole moments, particularly dipole moments (*e.g.* Coppens *et al.*, 1979; Moss, 1982), and exploration of concepts of charge and bonding in minerals (*e.g.* Sasaki, Fujino, Takeuchi & Sadanaga, 1980) and a range of organometallic, organic and inorganic compounds (*e.g.* Martin, Rees & Mitschler, 1982; Clemente, Biagini, Rees & Hermann, 1982).

The κ-refinement model yields chemically sensible atomic charges and sensible estimates of molecular properties such as the dipole moment. Formamide, for example, has been examined using a variety of techniques. The dipole moment determined from a κ refinement for formamide agrees well with values obtained by other experimental methods (Coppens *et al.*, 1979), and the individual atomic charges agree extremely well with those calculated from an *ab initio* wavefunction by fitting to the electrostatic potential (Chirlian & Francl, 1987). Stewart (1977) has demonstrated that the model electron-density function which best fits an observed electron density is the same model function which best fits the electrostatic potential, at least for data of unlimited resolution. It is because of this that the atomic charges obtained from a κ refinement based on X-ray diffraction data are physically reasonable, and hence they can sensibly be used to calculate the electrostatic potential within and around a molecule or crystal for use in modelling intermolecular interactions. This method is particularly attractive because of the great range and variety of molecules and crystals amenable to the κ-refinement procedure.

We are currently in the process of analysing X-ray diffraction data sets of varying qualities on several different zeolites, and because of limitations provided by the data and the large number of atoms in the asymmetric unit in several of these systems, it became clear to us that a simple monopole refinement procedure would be preferable to a full multipole model. Since we wish to use our results to investigate host–guest interactions in such systems, we decided to look more closely at the nature of the κ-refinement model. In particular, in this work we address the question of how closely κ-refined valence electron densities actually resemble real monopole deformations exhibited by atoms in molecules, and the implications this may have for the reliability of atomic charges and consequently the molecular properties calculated from them. Diatomic molecules containing first- and second-row atoms are used as models to obtain insight into the strengths and weaknesses of the κ-refinement model.

There are (at least) three approaches which could be taken in a model study of the κ-refinement procedure using diatomic molecular wavefunctions:

(i) The monopole generalized scattering factors (Stewart, Bentley & Goodman, 1975; Bentley & Stewart, 1975) (*i.e.* [0|0] GSFs) could be obtained for each diatomic and these atom-centred functions then κ refined in reciprocal space with appropriate atomic scattering factors.

(ii) The electron density in the molecule could be fitted directly with a κ-refinement model on both atoms in the molecule simultaneously, either in direct space or in reciprocal space. This is essentially what is done in the analysis of X-ray diffraction data, and

was the method pursued in earlier model studies on first-row diatomic hydrides (Chandler, Spackman & Varghese, 1980; Chandler & Spackman, 1982).

(iii) The deformation density could be partitioned into 'atomic' fragments, each of which may be spherically averaged, and the resulting single-atom electron densities fitted separately with a κ-refinement model.

For the present work we have adopted the latter approach, using the partitioning scheme devised by Hirshfeld (1977). This represents a compromise between the desire to use a procedure which is capable of generalization to polyatomic molecules [ruling out (i)], computationally straightforward [favouring (iii)], and as close as possible in principle to the analysis of X-ray diffraction data [favouring (i) or (ii)]. Our choice of (iii) introduces a particularly subtle bias: we are interested in modelling electrostatic properties, yet the Hirshfeld partitioning *at the monopole level* yields atomic charges which systematically underestimate molecular dipole moments by ~35% (Maslen & Spackman, 1985). We believe this is of minor consequence, as our aim is to analyse the monopole deformations associated with each atom, particularly those within ~2 Å of each nucleus. For this purpose the Hirshfeld partitioning of $\rho(\mathbf{r})$ should be entirely appropriate. We make no attempt to examine the adequacy of the electrostatic potential resulting from κ refinement of a model $\rho(\mathbf{r})$. That would require an approach more in line with (ii) above.

2. Method

Electron densities to be fitted by κ refinement were constructed for a number of diatomic molecules of first- and second-row elements in the following way. The total electron densities for the molecule, $\rho^{\rm mol}(\mathbf{r})$, and the promolecule, $\rho^{\rm pro}(\mathbf{r})=\sum_a \rho_a^{\rm atom}(\mathbf{r})$, were calculated directly from diatomic and atomic wavefunctions respectively (Clementi & Roetti, 1974; Cade & Huo, 1973, 1975; McLean & Yoshimine, 1967), and the deformation electron density, $\Delta\rho(\mathbf{r})$, obtained:

$$\Delta\rho(\mathbf{r})=\rho^{\rm mol}(\mathbf{r})-\rho^{\rm pro}(\mathbf{r}). \qquad (1)$$

The deformation density was then partitioned between the two atoms using the Hirshfeld partitioning scheme (Hirshfeld, 1977), in which the deformation density is apportioned to each atom in proportion to the electron density that atom contributes to the promolecular electron density.

$$\Delta\rho_a(\mathbf{r})=[\rho_a^{\rm atom}(\mathbf{r})/\rho^{\rm pro}(\mathbf{r})]\Delta\rho(\mathbf{r}), \qquad (2)$$

where $\Delta\rho_a(\mathbf{r})$ is the deformation density associated with atom a. Maslen & Spackman (1985) have shown that other quite disparate methods of partitioning the deformation electron density yield essentially the same results. The Hirshfeld partitioning is simple to apply and yields a smooth continuous $\Delta\rho_a(\mathbf{r})$. The deformation densities calculated *via* (2) are functions of three variables, denoted by the vector $\mathbf{r}$. The κ-refinement model, however, represents the best fit of a density function having spherical symmetry to an electron density generally having non-spherical symmetry. That is, the κ refinement is a fit to the spherical average of the electron density. This is accounted for here by numerical integration over angular coordinates, yielding a deformation density which is a function only of r_a, $\Delta\rho_a(r_a)$ (*i.e.* origin now at nucleus a).

The spherically averaged fragment electron density centred on nucleus a can be expressed as

$$\rho_a^{\rm mol}(r_a)=\rho_a^{\rm core}(r_a)+\rho_a^{\rm val}(r_a)+\Delta\rho_a(r_a), \qquad (3)$$

where $\rho_a^{\rm core}(r_a)$ and $\rho_a^{\rm val}(r_a)$ are the atomic core and valence electron densities respectively and $\Delta\rho_a(r_a)$ is the spherical average of (2). The last two terms in (3) comprise the monopole function which we fit in this work using the κ-refinement model (*i.e.* the 'observation'). It is constructed by adding the spherical atomic valence density to the deformation density previously calculated,

$$\rho_{\rm obs}(r)=\rho^{\rm val}(r)+\Delta\rho(r), \qquad (4)$$

where $\rho_{\rm obs}(r)$ is the 'observed' valence density of the atom in a given molecule, and the subscript a has been deleted for clarity.

The model electron density used to fit this function is

$$\rho_{\rm calc}(r)=P\kappa^3\rho^{\rm val}(\kappa r), \qquad (5)$$

where P is a variable population parameter allowing for charge transfer between atoms, κ scales the radial extent of the valence density, $\rho^{\rm val}(\kappa r)$ is the atomic valence density scaled by κ, and κ^3 is required to maintain normalization of $\rho^{\rm val}(\kappa r)$ to the number of valence electrons in the atom, $n^{\rm val}$ (see Coppens *et al.*, 1979).

Fitting the electron density in direct space and in reciprocal space are formally equivalent, subject to considerations such as the use of weighting schemes based on experimental uncertainties (Coppens & Hansen, 1977) and limitations on the extent of reciprocal-space data. The κ refinements performed in direct space in the present work are thus expected to yield essentially the same results as would be obtained with reciprocal-space fitting using extensive data sets.

Least-squares fits of $\rho_{\rm calc}(r)$ to $\rho_{\rm obs}(r)$ were performed by minimizing ε,

$$\begin{aligned}\varepsilon &= \int[\rho_{\rm obs}(\mathbf{r})-\rho_{\rm calc}(\mathbf{r})]^2\,{\rm d}\mathbf{r}\\ &= 4\pi\int_0^\infty[\rho_{\rm obs}(r)-\rho_{\rm calc}(r)]r^2\,{\rm d}r\\ &\simeq 4\pi\sum_i r_i^2[\rho_{\rm obs}(r_i)-\rho_{\rm calc}(r_i)]^2, \qquad (6)\end{aligned}$$

where the sum is taken over 400 evenly spaced intervals out to $r = 10$ a.u. It was found that, for all the diatomics studied, the atomic charges determined by numerical integration in this range were insignificantly different from those obtained by Maslen & Spackman (1985), who performed a numerical integration over r from zero to infinity by Gaussian quadrature. Values of the integrand in (6) for each of the diatomics were effectively zero at distances greater than 10 a.u. from the nucleus and hence numerical integration and least-squares fitting at distances greater than this was unnecessary.

3. Results

(i) *Deformation radial distribution (DRD) functions*

Although κ refinement is not a fit to the deformation density, but to a valence density which has been perturbed by the effects of bonding, it is more enlightening to examine how well the deformation density has been modelled by the κ refinement. Figs. 1 to 4 show the deformation radial distribution (DRD) function, $r^2\Delta\rho(r)$, for both atoms in each diatomic molecule, calculated by subtraction of $\rho_{val}(r)$ from both $\rho_{obs}(r)$ and $\rho_{calc}(r)$, and weighting of each point by r^2. This procedure serves two purposes. The first is that the functions which are plotted show directly the 'observed' deformation density and the deformation density calculated from a κ-refined valence density, both appropriately weighted to account for the spherical symmetry of the function. The second is that the plots are closely related to the net charge on the atoms,

$$q = -\int \Delta\rho(\mathbf{r})\,\mathrm{d}\mathbf{r} = -4\pi\int_0^\infty r^2\Delta\rho(r)\,\mathrm{d}r. \qquad (7)$$

That is, the area under the curve $r^2\Delta\rho(r)$ *vs* r is proportional to the net atomic charge. Note that the figures give plots of the functions for r out to 8 a.u. only, since they are negligibly different from zero at greater distances for most of the atoms.

The most striking feature evident in these plots is the generally excellent fits to the 'observed' functions provided by the κ-refinement procedure, especially considering that the κ-refinement model is such a simple two-parameter model. The best fits are observed for those diatomics in which there is a large deformation density (which integrates to give large charge transfer between atoms). Even for the poorer fits the general shape (*i.e.* positions of maxima and

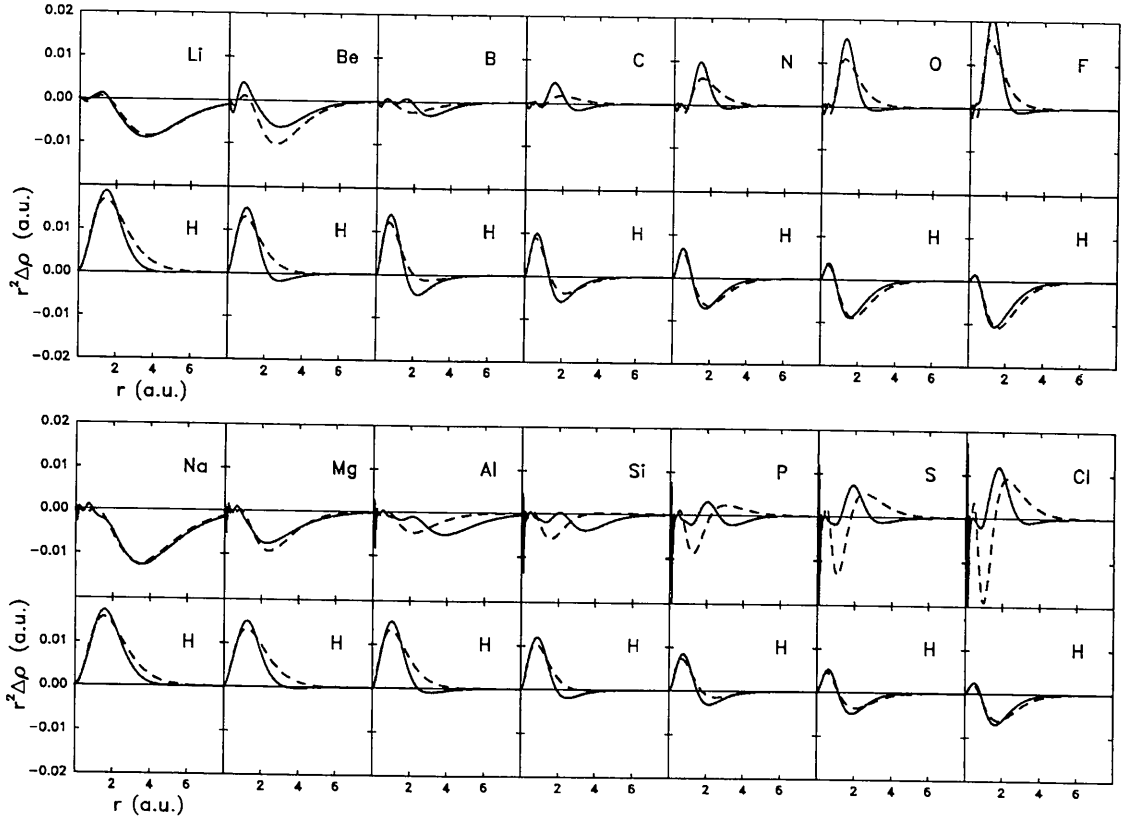

Fig. 1. Deformation radial distribution (DRD) functions, $r^2\Delta\rho(r)$, for the hydrides of the first- and second-row elements. Solid lines: 'observed' DRD functions. Dashed lines: DRD functions calculated from κ-refinement model.

minima, number of nodes *etc.*) of the calculated function mimics the general features of the 'observed' functions reasonably well, with only a few exceptions.

We note that the monopole deformation for each atom considered in this work must consist of contributions from each of the electron shells in the atom, although the usual approximation is that the core electron density remains undeformed in the bonded atom. Deformation of the inner-shell (K-shell) electron densities has been demonstrated for the first-row hydrides by Bentley & Stewart (1976) and Chandler & Spackman (1982). It is not unreasonable to expect significant L-shell deformations in second-row systems. The present model, however, modifies only the valence-electron-density function in an effort to fit the actual monopole deformations, and could therefore be expected to be less successful in fitting atoms which have significant core monopole deformations. This would appear to be the case for the second-row p-block atoms, for which large deformations are observed near the nucleus (within ~0·5 a.u.; see Fig. 1). The poorer fits of the model in these instances (*e.g.* heavy atoms in AlH, SiH, PH, SH, ClH, LiCl, NaCl) are probably due to the valence density

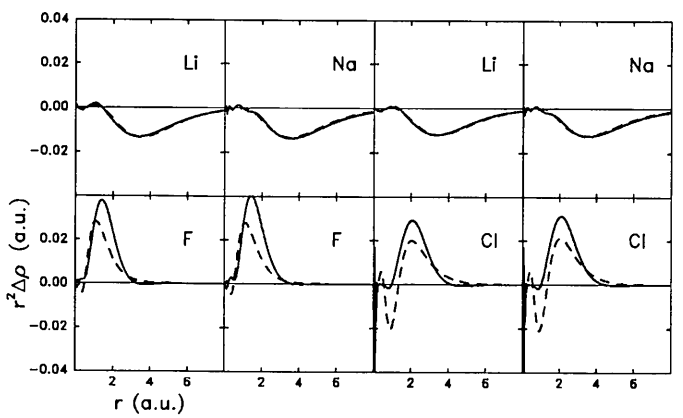

Fig. 2. Deformation radial distribution functions for selected alkali halides. Legend as for Fig. 1. Note that the vertical scale is twice that in Fig. 1.

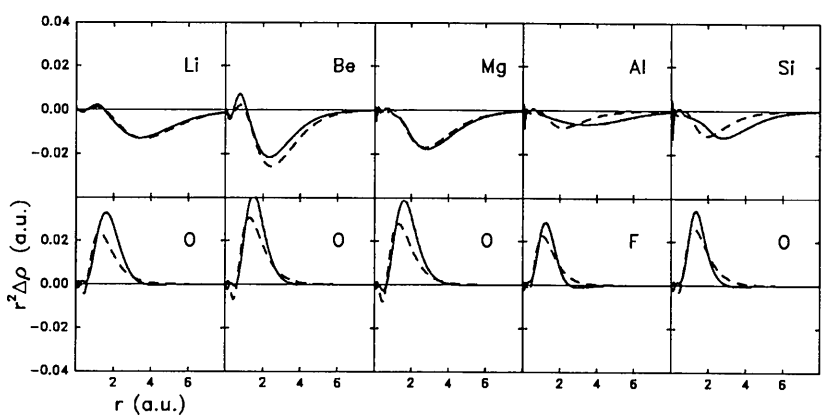

Fig. 3. Deformation radial distribution functions for selected oxides and an oxide analogue (AlF). Legend as for Fig. 1. Note that the vertical scale is twice that in Fig. 1.

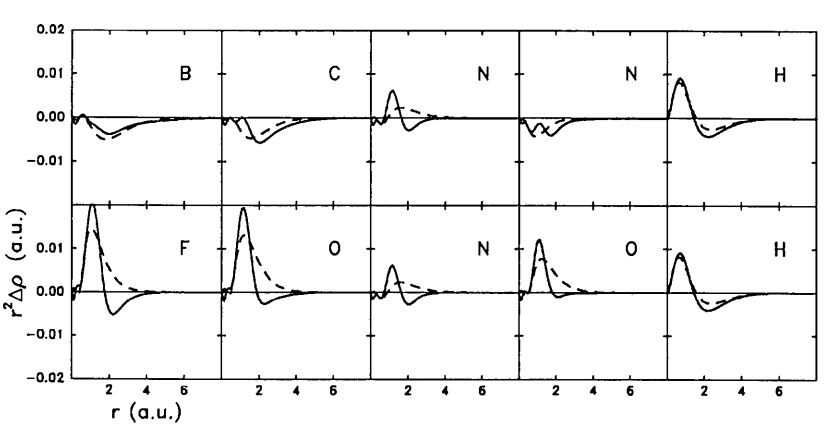

Fig. 4. Deformation radial distribution functions for several miscellaneous diatomics. Legend and scale as for Fig. 1.

functions having insufficient flexibility to fit the more complex deformation functions observed for these atoms.

The H atom in each of the first- and second-row hydrides (Fig. 1) and H_2 (Fig. 4) is very well modelled. Having no core electrons, hydrogen exhibits a monopole deformation which is due unequivocally to the effects of bonding on the valence electron density; its deformation density is relatively simple, having at most one node. It is noteworthy that hydrogen is well modelled in *each of a wide variety* of chemical environments which the first- and second-row hydrides represent. In particular, the DRD functions reflect in a very obvious way the electronegativity differences between each atom in the diatomic and also between the different first- and second-row elements. For example, the H atom in LiH has a net negative charge [positive $\int r^2\Delta\rho(r)\,dr$], while in FH the H atom has a net positive charge [negative $\int r^2\Delta\rho(r)\,dr$], with a smooth transition between these extremes through the intermediate hydrides.

Of all the cases examined, the atoms which are best modelled by the κ-refinement procedure are those for which the bonding is dominated by *s* electrons *i.e.* H and the *s*-block elements. Li and Na are particularly well modelled in LiH, LiO, LiF, LiCl, NaH, NaF and NaCl while Be and Mg in BeH, BeO, MgH and MgO are almost as good (Figs. 1–3). In each case the charge transfer is large and the DRD function relatively simple.

There are interesting qualitative similarities between the deformations exhibited by Na and Li in the more 'ionic' diatomics, particularly LiF, LiCl, LiO, NaF and NaCl. In each case the alkali-metal atom has a large rather simple deformation which is quite diffuse, peaking at 3 to 4 a.u. from the nucleus. It is remarkable how virtually identical deformations can be accommodated by the quite different Li 2*s* and Na 3*s* electron-density functions. O and F also display similarities in the 'ionic' diatomics, having large uncomplicated deformations peaking 1·5 to 2·0 a.u. from the nucleus.

There are qualitative differences for F in 'covalent' and 'ionic' diatomics. BF and FH represent 'covalent' environments in which F exhibits small relatively narrow deformations. In contrast, LiF and NaF represent more 'ionic' environments, in which the deformations of F are much larger and significantly broader than in BF and FH. O also shows such qualitative differences in its deformations in 'covalent' and 'ionic' diatomics, though the differences are less pronounced than for F.

(ii) *Net atomic charges*

The success of the κ-refinement procedure for determining net atomic charges is of course directly related to its success in reproducing the deformation density. The charge transfer from one atom to another is determined by the population parameter, *P*,

$$\Delta q_{\rm calc} = n^{\rm val}(P - 1{\cdot}0), \qquad (8)$$

where $\Delta q_{\rm calc}$ is the *electron* transfer from the atom in question and $n^{\rm val}$ is the number of valence electrons in the isolated atom. Note that $\Delta q_{\rm calc}$ refers to the transfer of negative charge (*i.e.* electrons), so that a positive $\Delta q_{\rm calc}$ indicates that an atom has a net negative electrical charge. Table 1 compares the charge transfer for each atom calculated from the κ-refined population parameter with that calculated by integration of the partitioned deformation density (*i.e.* the 'observed' net charge on each atom).

Table 1. *Kappas and charge transfers, Δq_{calc} (in electrons), from κ refinement of $\Delta\rho_a(\mathbf{r})$ spherically averaged about the nuclear position of atom a*

'Observed' charge transfer values, $\Delta q_{\rm obs}$, are from integration of the partitioned deformation density (Maslen & Spackman, 1985), and are given only for the second atom in each diatomic.

Diatomic	κ	$\Delta q_{\rm calc}$	$\Delta q_{\rm obs}$	Diatomic	κ	$\Delta q_{\rm calc}$	$\Delta q_{\rm obs}$
Li	1·129	−0·407		Li	1·249	−0·607	
H	0·907	+0·491	+0·414	O	0·972	+0·420	+0·581
Be	1·048	−0·348		Be	1·136	−0·854	
H	1·020	+0·275	+0·193	O	0·962	+0·534	+0·646
B	1·005	−0·069		Mg	1·025	−0·644	
H	1·100	+0·134	+0·075	O	0·963	+0·480	+0·678
C	0·994	+0·036		Al	0·998	−0·243	
H	1·144	−0·002	−0·016	F	0·981	+0·357	+0·357
N	0·989	+0·115		Si	1·001	−0·320	
H	1·171	−0·105	−0·091	O	0·971	+0·468	+0·461
O	0·987	+0·192		Li	1·214	−0·629	
H	1·183	−0·183	−0·164	F	0·974	+0·448	+0·620
F	0·986	+0·252		Na	1·057	−0·652	
H	1·182	−0·266	−0·228	F	0·974	+0·441	+0·677
Na	1·061	−0·400		Li	1·138	−0·566	
H	0·892	+0·467	+0·413	Cl	0·966	+0·301	+0·551
Mg	0·984	−0·304		Na	1·025	−0·598	
H	0·957	+0·356	+0·282	Cl	0·965	+0·322	+0·617
Al	0·999	−0·150		B	1·008	−0·141	
H	1·003	+0·305	+0·228	F	0·988	+0·231	+0·118
Si	0·990	−0·096		C	1·006	−0·112	
H	1·049	+0·174	+0·125	O	0·987	+0·234	+0·139
P	0·984	−0·040		N	0·994	+0·040	
H	1·080	+0·056	+0·034	N	0·994	+0·040	0·000
S	0·979	+0·012		N	0·998	−0·065	
H	1·104	−0·048	−0·050	O	0·991	+0·138	−0·086
Cl	0·976	+0·049		H	1·110	+0·031	
H	1·122	−0·139	−0·124	H	1·110	+0·031	0·000

As one would expect from the consideration of the DRD functions, the net atomic charges determined by κ refinement generally agree very well with those 'observed' particularly for those diatomics for which charge transfer is relatively large. The least-successful cases are those atoms which have the more complicated structure in their DRD functions, most notably the second-row *p*-block elements. The problem is again related to the inability of the valence density functions to reproduce the more highly structured deformation densities in these diatomics. However, for the cases where the deformation density is small (and the DRD functions do not reproduce the shape of the deformation very well) the charges which are

obtained by κ refinement are still remarkably good. For example, B and C in BH and CH have net charges of $-0{\cdot}069$e and $+0{\cdot}036$e respectively compared with the 'observed' charges of $-0{\cdot}075$e and $+0{\cdot}016$e.

It is worth emphasizing that the 'observed' charge transfer in this work is always less than one electron, even for examples such as NaCl where one might expect the transfer of one electron from the Na to the Cl. This result stems from the partitioning of the deformation density *via* (2) in the construction of an 'observed' valence density. Maslen & Spackman (1985) have discussed how the Hirshfeld scheme must yield charge transfers which are lower than expected for cation–anion pairs, and note that there is no partitioning scheme which can retrieve all of the expected charge transfer from the deformation density. What is important here is that, given a particular charge transfer, the κ-refinement procedure is able to give a very good estimate *of that* charge transfer.

(iii) *Kappas*

The κ values obtained (Table 1) are correlated with the charge transfer as expected from the work of Coppens *et al.* (1979). That is, atoms having a net negative charge (positive charge transfer) have valence shells which are expanded relative to the isolated atom ($\kappa < 1{\cdot}0$) while atoms having a net positive charge (negative charge transfer) have valence shells contracted relative to the isolated atom ($\kappa > 1{\cdot}0$). The exceptions to this are N_2, NO, MgH and AlF, where the valence shells of both atoms in each diatomic are marginally more diffuse than in the isolated atoms, BeH and BH where both are slightly contracted, and H_2 in which H is significantly contracted but there is no charge transfer. The greatest effect is observed for the Li atom in LiO, where there is a 24·9% ($\kappa = 1{\cdot}249$) contraction of the valence-electron density on Li relative to the isolated atom.

It is worthwhile comparing the range of κ values obtained in the present work with energy-optimized scale factors for atoms in polyatomic hydrides, obtained with Gaussian expansions (STO-NG) of Slater-type orbitals (Hehre, Stewart & Pople, 1969; Hehre, Ditchfield, Stewart & Pople, 1970). For example, for H in CH_4, NH_3, H_2O and HF, the energy-optimized exponents are 1·16, 1·23, 1·26 and 1·32, respectively, generally larger than the present values of 1·144, 1·171, 1·183 and 1·182 for the diatomic hydrides. The second-row systems were treated in more detail by those authors and, for H bonded to Na through Cl, the energy-optimized exponent ranges from 0·77 (NaH) to 1·20 (HCl); the κ-refined values obtained from diatomic molecules display similar behaviour, but span a narrower range, 0·892 (NaH) to 1·122 (HCl). It is also possible to deduce energy-optimized κ values for heavy atoms from the atomic and molecular energy-optimized exponents reported by Hehre and co-workers (Hehre, Stewart & Pople, 1969; Hehre, Ditchfield, Stewart & Pople, 1970). As noted for H above, these energy-optimized values display the same trends as, but often more exaggerated than, the κ-refined (density-fitted) values. For example, for the heavy atoms Na to Cl, Hehre *et al.* obtained scale factors of 1·40 (NaH), 1·43 (MgH_2), 1·26 (AlH_3), 1·18 (SiH_4), 1·04 (PH_3), 1·02 (H_2S) and 1·00 (HCl), compared with κ-refined values of 1·061 (NaH), 0·984 (MgH), 0·999 (AlH), 0·990 (SiH), 0·984 (PH_3), 0·979 (H_2S) and 0·976 (HCl). The two different estimates of valence expansion and contraction upon bonding both suggest that the effect is small in covalent molecules, and larger in ionic species, and typically less than 20%. However, energy optimization weights the region near the nucleus heavily, whereas electron-density-fitting procedures such as κ refinement depend more strongly on regions further from the nucleus. Energy-optimized exponents (kappas) are not necessarily appropriate for use in least-squares fitting of the electron density.

The electron densities which have been constructed here are completely free of thermal motion, and the nuclear positions are known exactly. There can be no possibility of correlations between the κ-refinement parameters (particularly κ) and a thermal vibration parameter, U, nor is there any doubt as to the location of the proton in the hydride series. Both of these complications must be considered in any analysis of X-ray data. In the absence of these complicating effects, the H atom in the hydride series exhibits a maximum contraction of 18·2% ($\kappa = 1{\cdot}182$) in FH and a maximum expansion of 10·8% ($\kappa = 0{\cdot}892$) in LiH. These magnitudes are in excellent agreement with values obtained by Stewart, Davidson & Simpson, (1965) and Chandler *et al.* (1980), who obtained kappas of 1·166 and 1·126 respectively in monopole fits to an H_2 electron-density function beyond the Hartree–Fock limit. They are at variance with the work of Coppens *et al.* (1979) who advocate $\kappa = 1{\cdot}40$ for H atoms. The latter work involves thermal motion and H atom positions as variables but it is not clear that those complications should affect κ substantially. A 40% contraction of the H-atom electron density seems extremely large in the light of both the present work and the energy-optimized values of typically 15 to 20% for a C—H bond.

A referee has suggested that spherical averaging of $\Delta\rho_a(\mathbf{r})$ with respect to the centroid of $\rho_a^{\rm mol}(\mathbf{r})$, rather than the nuclear position, may highlight reasons for this discrepancy. To investigate this point we have spherically averaged $\Delta\rho_a(\mathbf{r})$ about the centroid of $\rho_a^{\rm mol}(\mathbf{r})$, z_a, $[z_a = \int z\rho_a^{\rm mol}(\mathbf{r})\,d\mathbf{r} / \int \rho_a^{\rm mol}(\mathbf{r})\,d\mathbf{r}]$ for the first-row hydrides, and subsequently κ refined the resulting spherical valence electron densities. The results are presented in Table 2. It is clear that the

Table 2. *Kappas and charge transfers from κ refinement of $\Delta\rho_a(\mathbf{r})$ spherically averaged about the centroid of $\rho_a^{mol}(\mathbf{r})$, z_a (see text)*

z_a is in Å, the positive z direction being from heavy atom to H in each case. $\%\Delta\kappa$ is the percent difference between the kappas obtained in fits to $\rho_a^{val}(\mathbf{r})$ spherically averaged about the nucleus of atom a (Table 1) and about the centroid of $\rho_a^{mol}(\mathbf{r})$ (this table). Other quantities are as for Table 1.

Diatomic	z_a	κ	$\%\Delta\kappa$	Δq_{calc}	Δq_{obs}
H	+0·076	1·137	+2·4	+0·021	
H	−0·076	1·137	+2·4	+0·021	0·000
Li	+0·236	1·343	+19·0	−0·528	
H	−0·016	0·909	+0·2	+0·490	+0·414
Be	−0·042	1·047	−0·1	−0·320	
H	−0·033	1·028	+0·8	+0·270	+0·193
B	−0·085	1·016	+1·1	−0·098	
H	−0·043	1·114	+1·3	+0·126	+0·075
C	−0·040	0·999	+0·5	+0·007	
H	−0·068	1·168	+2·1	−0·013	−0·016
N	−0·021	0·991	+0·2	+0·096	
H	−0·104	1·203	+2·7	−0·113	−0·091
O	−0·011	0·981	−0·6	+0·180	
H	−0·147	1·220	+3·1	−0·193	−0·164
F	−0·006	0·987	+0·1	+0·247	
H	−0·185	1·222	+3·4	−0·249	−0·228

centroid of $\rho_a^{mol}(\mathbf{r})$ for H is significantly shifted from the position of the proton, always into the bond, typically by ~0·07 Å (for H_2 and CH) and by as much as 0·19 Å (for FH). Nevertheless, the resulting kappas for H are only marginally larger (~2 to 3%) than values in Table 1. Our results echo those obtained by Stewart *et al.* (1965) who found that the 'best' monopole fit to the H_2 molecule electron density was centred 0·070 Å into the bond (*cf.* $z_a = 0{\cdot}076$ Å for H_2 in Table 2 of the present work). That work also reports that the contraction of the H 1*s* orbital upon bonding 'is about the same whether the spherical density is centred about the proton or floated off to an optimal position'. Apparently, the discrepancy between κ values for H obtained from experiment and in model studies such as the present one cannot be explained solely in terms of the apparent movement of the proton into the bond. This matter deserves further attention, in model studies which must deal explicitly with factors such as nuclear positions, thermal motion, and probably the resolution of the X-ray data.

We note that, with the exception of Li in LiH, the centroid of the heavy atom $\rho_a^{mol}(\mathbf{r})$ is outside the bond. The effect on κ, however, is even smaller than that observed for H above. The centroid of $\rho_{Li}^{mol}(\mathbf{r})$ in LiH is 0·24 Å towards the proton, seemingly at variance with other results in Table 2. This is a direct consequence of the extremely diffuse Li 2*s* orbital, which results in apportioning most of $\rho^{mol}(\mathbf{r})$, except in the immediate vicinity of the proton, to $\rho_{Li}^{mol}(\mathbf{r})$. In a sense it is an artefact of the Hirshfeld partitioning procedure, leading to a large shift of the centroid from the nuclear position, and hence a large change in κ.

Coppens *et al.* (1979) have noted the difficulty associated with charge-density refinement of X-ray diffraction data for the alkali halides. Because of the diffuseness of the valence electron density in the alkali metals, in a typical X-ray data set there are few reflections which are affected by scattering by the valence electrons of these atoms, with the result that refinement of population and scaling parameters (P and κ) usually leads to very poorly determined κ values. In the present work the charges and kappas for the alkali metals in the alkali halides are very well determined, although dependent on the particular model used in their derivation; use of the present kappas in refinements with X-ray data may be worthwhile.

4. Concluding remarks

Monopole deformations experienced by atoms in molecules can be well modelled by radially expanded or contracted atomic valence-electron-density functions with a modified population. The κ-refinement model is a particularly simple one and is less demanding of the data than the more sophisticated multipole models which are available for charge density analysis (*e.g.* Stewart; 1973, 1976). Nevertheless, the κ-refinement procedure applied to the diatomics in this work is capable of reproducing, with surprising success, the monopole deformations and consequently the net charges on atoms in those molecules.

The present model study differs from the normal application of the κ-refinement strategy to X-ray diffraction data in several important respects. It has been restricted to separately fitting the Hirshfeld partitioned-atom centred monopole deformations obtained from near Hartree–Fock quality wavefunctions. In particular, the strategy we have chosen is not directly comparable to a multicentre κ refinement based on X-ray diffraction data, especially when bearing in mind additional factors such as data-set resolution and thermal motion which are encountered in experimental electron-density studies. Nevertheless, we believe that, with the possible exception of hydrogen, the major conclusions are valid and applicable to the analysis of experimental data and would not be substantially altered by modifying our simple approach.

References

BENTLEY, J. & STEWART, R. F. (1975). *J. Chem. Phys.* **63**, 3794–3803.

BENTLEY, J. & STEWART, R. F. (1976). *Acta Cryst.* A**32**, 910–914.

CADE, P. E. & HUO, W. (1973). *At. Data Nucl. Data Tables*, **12**, 415–466.

CADE, P. E. & HUO, W. (1975). *At. Data Nucl. Data Tables*, **15**, 1–39.

CHANDLER, G. S. & SPACKMAN, M. A. (1982). *Acta Cryst.* A**38**, 225–239.

CHANDLER, G. S., SPACKMAN, M. A. & VARGHESE, J. N. (1980). *Acta Cryst.* A**36**, 657–669.

CHIRLIAN, L. E. & FRANCL, M. M. (1987). *J. Comput. Chem.* **8**, 894-905.
CLEMENTE, D. A., BIAGINI, M. C., REES, B. & HERMANN, W. A. (1982). *Inorg. Chem.* **21**, 3741-3749.
CLEMENTI, E. & ROETTI, C. (1974). *At. Data Nucl. Data Tables*, **14**, 177-478.
COPPENS, P. (1989). *J. Phys. Chem.* **93**, 7979-7984.
COPPENS, P., GURU ROW, T. N., LEUNG, P., STEVENS, E. D., BECKER, P. J. & YANG, Y. W. (1979). *Acta Cryst.* A**35**, 63-72.
COPPENS, P. & HANSEN, N. K. (1977). *Isr. J. Chem.* **16**, 163-167.
COPPENS, P., PAUTLER, D. & GRIFFIN, J. F. (1971). *J. Am. Chem. Soc.* **93**, 1051-1058.
HEHRE, W. J., DITCHFIELD, R., STEWART, R. F. & POPLE, J. A. (1970). *J. Chem. Phys.* **52**, 2769-2773.
HEHRE, W. J., STEWART, R. F. & POPLE, J. A. (1969). *J. Chem. Phys.* **51**, 2657-2664.
HIRSHFELD, F. L. (1977). *Theor. Chim. Acta*, **44**, 129-138.
MCLEAN, A. D. & YOSHIMINE, M. (1967). *Tables of Linear Molecule Wave Functions. IBM J. Res. Dev.* Supplement, November 1967.
MARTIN, M., REES, B. & MITSCHLER, A. (1982). *Acta Cryst.* B**38**, 6-15.
MASLEN, E. N. & SPACKMAN, M. A. (1985). *Aust. J. Phys.* **38**, 273-287.
MOSS, G. (1982). In *Electron Distributions and the Chemical Bond*, edited by P. COPPENS & M. B. HALL, pp. 383-411. New York: Plenum Press.
PEARLMAN, D. A. & KIM, S. H. (1985). *Biopolymers*, **24**, 327-357.
SASAKI, S., FUJINO, K., TAKEUCHI, Y. & SADANAGA, R. (1980). *Acta Cryst.* A**36**, 904-915.
STEWART, R. F. (1970). *J. Chem. Phys.* **53**, 205-213.
STEWART, R. F. (1973). *J. Chem. Phys.* **58**, 1668-1676.
STEWART, R. F. (1976). *Acta Cryst.* A**32**, 565-574.
STEWART, R. F. (1977). *Isr. J. Chem.* **16**, 124-131.
STEWART, R. F., BENTLEY, J. & GOODMAN, B. (1975). *J. Chem. Phys.* **63**, 3786-3793.
STEWART, R. F., DAVIDSON, E. R. & SIMPSON, W. T. (1965). *J. Chem. Phys.* **42**, 3175-3187.
YANEZ, M. & STEWART, R. F. (1978). *Acta Cryst.* A**34**, 648-651.
YANEZ, M., STEWART, R. F. & POPLE, J. A. (1978). *Acta Cryst.* A**34**, 641-648.

Acta Cryst. (1991). A**47**, 29-36

Niggli Lattice Characters: Definition and Graphical Representation

BY P. M. DE WOLFF

Vakgroep VS-FK, Laboratorium vor Technische Natuurkunde, TU Delft, Lorentzweg 1, *Postbus* 5046, 2600 *GA Delft, The Netherlands*

AND B. GRUBER

Faculty of Mathematics and Physics, Charles University, Malostranské nám. 25, 11800 *Prague* 1, *Czechoslovakia*

(*Received* 24 *April* 1990; *accepted* 21 *August* 1990)

Abstract

An exact definition of the 44 lattice characters listed by Niggli is thoroughly discussed and is elucidated by examples. In order to represent the characters graphically, use is made of the projection of the Niggli-reduced basis vector **c** on the **a**, **b** plane. Not only is the projected end point of **c** restricted to certain domains in the plane by the reduction rules - *cf. International Tables for Crystallography* (1987), Chapter 9.3 (Dordrecht: Kluwer) - but for given constants A, B and F in the Niggli-reduced form this polygonal domain contains the locus of each of the characters as a vertex or an edge or the area of the polygon. For each of the cases $a = b = c$, $a = b < c$, $a < b = c$ and $a < b < c$, nine figures fully cover all alternatives determined by five special values $F = A/2$, 0, $-A/4$, $-A/3$ and $-A/2$ and the four open intervals between them. Also, all normalized Buerger bases which are not Niggli-reduced bases are shown in the same figures.

1. Introduction

It has been shown (*International Tables*, 1987, referred to as *IT*87 hereafter) that the reduced basis of any given crystal lattice can be elucidated graphically by the perpendicular projection of the reduced basis vector **c** upon the **a**, **b** plane. Because of the rules for cell reduction, only points within certain regions in that plane are allowed as a possible projected end point of **c**, **a** and **b** being considered as given vectors. Drawings of the **a**, **b** plane, showing these regions for only a limited number of typical cases, fully illustrate all rules of cell reduction.

The reduced cell which we here refer to is the cell introduced by Niggli (1928). Since some other types of reduced cell have been discussed recently (Gruber, 1989), we shall denote it further as the 'Niggli cell', and its normalized basis as the 'Niggli basis'.

Closely related to Niggli cells are the lattice characters, which constitute a classification of lattices based mainly on lattice symmetry expressed in the

0108-7673/91/010029-08$03.00